

Octadecanuclear Cluster or 1D Polymer with $\{ML\}_2Nb(CN)_8\}_n$ Motifs as a Function of $\{ML\}$ ($M = Ni(II)$, $n = 6$; $M = Mn(II)$, $n = \infty$; $L =$ Macrocycle)

Rabindranath Pradhan, Cédric Desplanches, Philippe Guionneau, and Jean-Pascal Sutter*

Institut de Chimie de la Matière Condensée de Bordeaux—CNRS, 87 Avenue Dr. Schweitzer, F-33608 PESSAC, France

Received June 6, 2003

A nanosized octadecaheteronuclear aggregate, $[\{NiL^2\}_{12}\{Nb(CN)_8\}_6(H_2O)_6]$, and a 1-D coordination polymer, $[\{MnL^1\}_2\{Nb(CN)_8\}_2(H_2O)]_\infty$, have been obtained by self-assembly between the octacyanometalate $\{Nb(CN)_8\}^{4-}$ and $\{ML\}^{2+}$ complexes. The dimensionality of the supramolecular architectures was found to be controlled by the $\{ML\}$ module for which the equatorial coordination sites are blocked by a macrocyclic ligand. The crystal structures and magnetic properties for both the compounds are described.

The design of supramolecular materials prepared from molecular building blocks has become a challenging field of research which opens new perspectives in material science. A versatile approach to heterometallic systems consists of assembling complementary molecular modules by means of a bridging ligand. A prominent example of this synthetic strategy is found in the preparation of magnets based on the Prussian blue type framework.¹ When cyanometalate derivatives are used for the preparation of high-nuclearity metal ion clusters, additional “capping” ligands are usually required to prevent the formation of an extended coordination network.^{2–5} So far, most of such molecular aggregates are based on paramagnetic 3d ions, and only very few examples involving ions from the second or third transition metal series have been reported.^{6–10} The latter ions, however, proved

recently in extended networks to be very appealing spin carriers.^{11,12}

In the present report, we show that the association of an octacyanometalate module with a $\{ML\}$ unit, in which the equatorial coordination sites are blocked, might be an alternative and efficient approach to high-nuclearity coordination clusters. We disclose the structures of an octadecanuclear aggregate and a 1D coordination polymer obtained with $\{Nb(CN)_8\}^{4-}$. Interestingly, the resulting supramolecular architecture is directed by the second partner of the reaction.

When $\{Nb(CN)_8\}^{4-}$ is reacted in H_2O solutions with $\{MnL^1\}^{2+}$ or $\{NiL^2\}^{2+}$ units where L^1 and L^2 stand for a macrocyclic ligand occupying the equatorial coordination sites (Chart 1), the spontaneous assembling leads to crystalline compounds of elementary composition $[\{ML\}_2\{Nb(CN)_8\}]_n \cdot xH_2O$ identified hereafter as **1** for $M = Mn$ and **2** for $M = Ni$.²⁰

The single-crystal X-ray structure determination revealed that **1**²¹ has a 1-D polymeric structure based on the alternation of $\{Nb(CN)_8\}$ and $\{MnL^1\}$ units. It is isomorphous to the compound formed with $\{MnL^1\}$ and $\{Mo(CN)_8\}^{4-}$.¹³ Each $\{Nb(CN)_8\}$ module is linked to three $\{MnL^1\}$ moieties through $NbCN \rightarrow Mn$ linkages. Two of these $\{MnL^1\}$ units accommodate further Nb modules in trans position, thus

* To whom correspondence should be addressed. E-mail: jpsutter@icmcb.u-bordeaux.fr.

- (1) Verdager, M.; Bleuzen, A.; Marvaud, V.; Vaissermann, J.; Seuleiman, M.; Desplanches, C.; Scuille, A.; Train, C.; Garde, R.; Gelly, G.; Lomenech, C.; Rosenman, I.; Veillet, P.; Cartier, C.; Villain, F. *Coord. Chem. Rev.* **1999**, *190–192*, 1023–47.
- (2) Mallah, T.; Marvilliers, A. In *Magnetism: molecules to materials*; Miller, J. S., Drillon, M., Ed.; Wiley-VCH: Weinheim, 2001; Vol. 2, pp 189–226.
- (3) Marvaud, V.; Decroix, C.; Scuille, A.; Guyard-Duhayon, C.; Vaissermann, J.; Gonnet, F.; Verdager, M. *Chem. Eur. J.* **2003**, *9*, 1678–91.
- (4) Marvaud, V.; Decroix, C.; Scuille, A.; Tuyères, F.; Guyard-Duhayon, C.; Vaissermann, J.; Marrot, J.; Gonnet, F.; Verdager, M. *Chem. Eur. J.* **2003**, *9*, 1692–1705.
- (5) Yang, J. Y.; Shores, M. P.; Sokol, J. J.; Long, J. R. *Inorg. Chem.* **2003**, *42*, 1403–19.

- (6) Zhong, Z. J.; Seino, H.; Mizobe, Y.; Hidai, M.; Fujishima, A.; Ohkoshi, S.-I.; Hashimoto, K. *J. Am. Chem. Soc.* **2000**, *122*, 2952–3.
- (7) Larionova, J.; Gross, M.; Pilkington, M.; Andres, H.; Stoeckli-Evans, H.; Güdel, H. U.; Decurtins, S. *Angew. Chem., Int. Ed.* **2000**, *39*, 1605–9.
- (8) Podgajny, R.; Desplanches, C.; Sieklucka, B.; Sessoli, R.; Villar, V.; Paulsen, C.; Wernsdorfer, W.; Dromzée, Y.; Verdager, M. *Inorg. Chem.* **2002**, *41*, 1323–7.
- (9) Sokol, J. J.; Hee, A. G.; Long, J. R. *J. Am. Chem. Soc.* **2002**, *124*, 7656–7.
- (10) Bonadio, F.; Gross, M.; Stoeckli-Evans, H.; Decurtins, S. *Inorg. Chem.* **2002**, *41*, 5891–6.
- (11) Mathonière, C.; Sutter, J.-P.; Yakhmi, J. V. In *Magnetism: molecules to materials*; Miller, J. S., Drillon, M., Ed.; Wiley-VCH: Weinheim, 2002; Vol. 4, pp 1–40.
- (12) Tanase, S.; Tuna, F.; Guionneau, P.; Maris, T.; Rombaut, G.; Mathonière, C.; Andruh, M.; Kahn, O.; Sutter, J.-P. *Inorg. Chem.* **2003**, *42*, 1625–31.
- (13) Rombaut, G.; Golhen, S.; Ouahab, L.; Mathonière, C.; Kahn, O. *J. Chem. Soc., Dalton Trans.* **2000**, 3609–14.

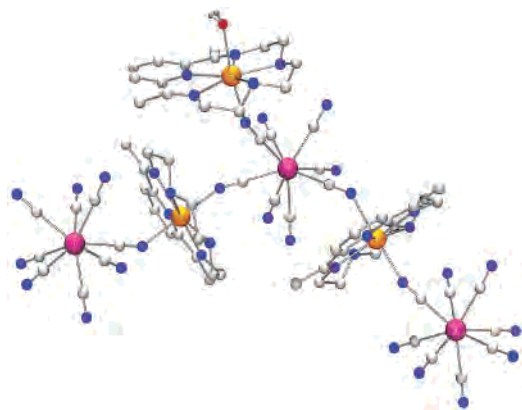
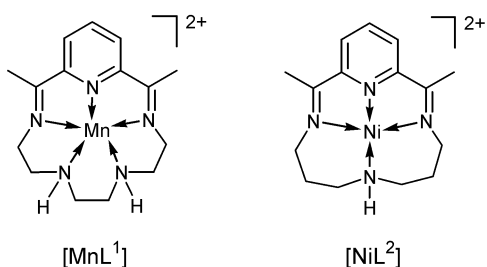


Figure 1. Detail of the chain structure developing along *c*-axis for $\{[MnL^1]_2\{Nb(CN)_8\}(H_2O) \cdot 5H_2O\}_\infty$, **1**. H atoms and lattice H_2O molecules are omitted.

Chart 1



developing the coordination polymer. The remaining $\{MnL^1\}$ unit is terminal, and its coordination sphere is completed by a H_2O ligand. A view of this arrangement is given in Figure 1. The crystal lattice is completed by five H_2O molecules leading for compound **1** to the formula $\{[MnL^1]_2\{Nb(CN)_8\}(H_2O) \cdot 5H_2O\}_\infty$.

The single-crystal X-ray structure determination for Ni derivative **2**²¹ revealed a similar elementary association pattern; i.e., each $\{Nb(CN)_8\}$ module is linked to three $\{NiL^2\}$ units, one of them is terminal whereas two act as bridges between Nb centers, but the supramolecular object is now found to be a $\{[NiL^2]_{12}\{Nb(CN)_8\}_6\}$ aggregate (Figure 2). The latter can be described as an hexagon in a chair conformation consisting of six $\{Nb(CN)_8\}$ modules bridged by six $\{NiL^2\}$ units; the Nb atoms are located on the vertexes, and the Nb–CN→Ni←NC–Nb linkages form the sides. The remaining six terminal $\{Ni(H_2O)L^2\}$ units act as axial substituents of this giant cyclohexane-type arrangement. An idea of the size of this molecule is given by the distance of 30 Å between the O atoms of the Ni(H_2O) centers located at opposite edges (1,4 substituents). The crystal lattice contains a very large number of diffuse water molecules that cannot be located by X-ray diffraction analysis. The H_2O content was provided by the chemical and TG analyses indicating that 100 H_2O molecules in addition to the coordinated molecules are present per aggregate leading to the formula $\{[NiL^2]_{12}\{Nb(CN)_8\}_6(H_2O)_6\} \cdot 100H_2O$ for **2**.

The magnetic properties for these compounds were investigated in the temperature domain 2–300 K. For compound **1**, the value of $\chi_M T$ (where χ_M stands for the molar magnetic susceptibility) at 300 K is $8.85 \text{ cm}^3 \text{ K mol}^{-1}$, in good agreement with the spin-only value of $9.125 \text{ cm}^3 \text{ K}$

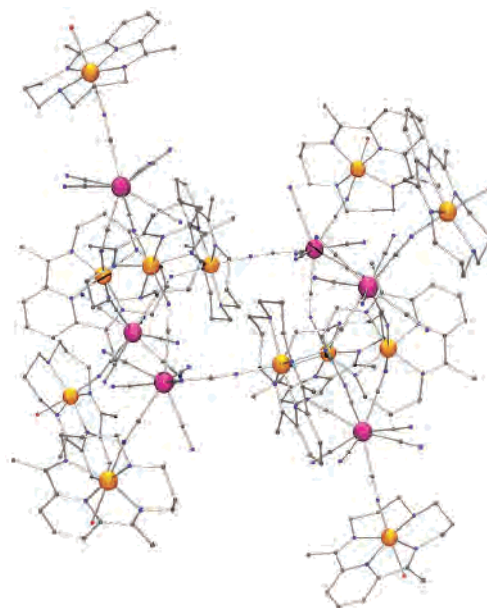


Figure 2. View of the molecular structure for $\{[NiL^2]_{12}\{Nb(CN)_8\}_6(H_2O)_6\}$, **2**. H atoms and lattice H_2O molecules are omitted.

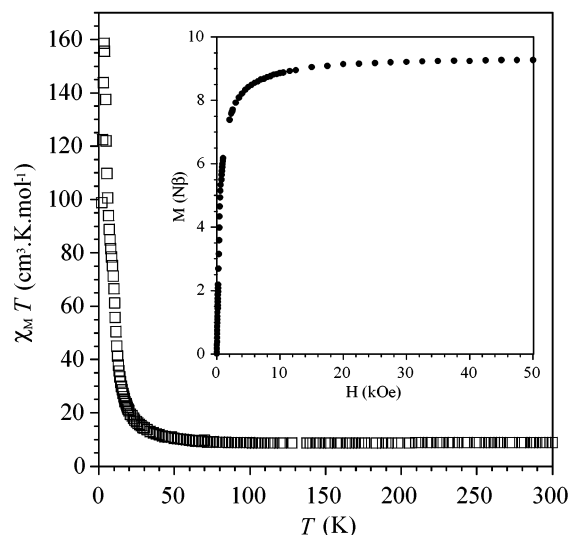


Figure 3. Temperature dependence of $\chi_M T$ for $\{[MnL^1]_2\{Nb(CN)_8\}(H_2O) \cdot 5H_2O\}_\infty$, **1**. Insert shows field dependence of the magnetization at 2 K.

mol^{-1} anticipated for two Mn(II) ions ($S = 5/2$) and one Nb(IV) ion ($S = 1/2$), and slowly decreases on cooling to 130 K. For lower T , the value of $\chi_M T$ rises more and more rapidly suggesting long-range magnetic correlation among the spin carriers (Figure 3). The field cooled magnetization ($H = 50$ Oe) down to 2 K exhibits the onset of a plateau suggesting magnetic order. But when the field was switched off at this temperature, no remnant magnetization was observed. The field dependence of the magnetization recorded at 2 K (Figure 3 insert) indicates that **1** quickly reaches a saturation magnetization of $9 N\beta$. This value suggests that the {Mn–Nb} interaction is antiferromagnetic. The analysis by the Curie–Weiss equation of the linear part of the $1/\chi_M$ versus T curve (150–300 K) for this compound yielded $C = 9.10 \text{ cm}^3 \text{ K mol}^{-1}$ and $\theta = -8.4 \text{ K}$.

The magnetic behavior exhibited by compound **2** is depicted in Figure 3 as $\chi_M T$ versus T plot. At 300 K, the

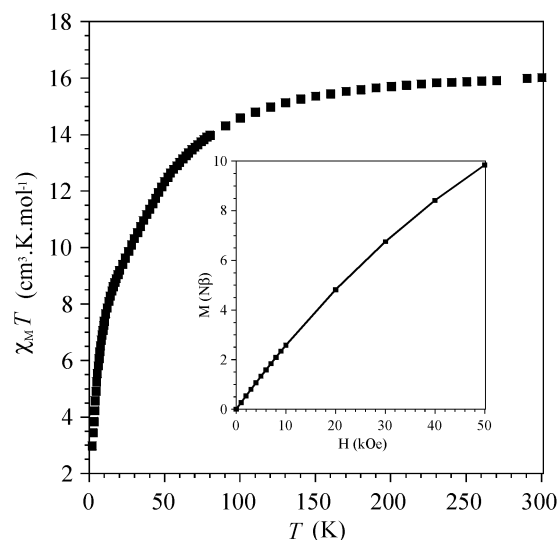


Figure 4. Temperature dependence of $\chi_M T$ for $\{[\text{NiL}^2]_{12}\{\text{Nb}(\text{CN})_8\}_6 \cdot (\text{H}_2\text{O})_6\}$, **2**. Insert shows field dependence of the magnetization at 2 K.

value for $\chi_M T$ is $16.0 \text{ cm}^3 \text{ K mol}^{-1}$, a value in good agreement with $15.5 \text{ cm}^3 \text{ K mol}^{-1}$ expected for 12 Ni(II) ($S = 1$, $g = 2.10$) and 6 Nb(IV) ($S = 1/2$, $g = 2$). This value was found to decrease more and more rapidly when T was lowered to reach $3 \text{ cm}^3 \text{ K mol}^{-1}$ for 2 K. Such behavior is rather surprising for a compound where 12 $S = 1$ spin carriers interact with 6 $S = 1/2$ centers. Indeed, ferromagnetic $\{\text{Ni}-\text{Nb}\}$ interactions should lead to a spin ground state of $S = 15$ whereas a $S = 9$ spin state is the result of antiferromagnetic interactions; in both cases, $\chi_M T$ should increase to reach, respectively, values close to 120 and $45 \text{ cm}^3 \text{ K mol}^{-1}$ at low temperature. The magnetic behavior found for **2** suggests that overall antiferromagnetic interactions are operative in the crystal lattice. The field dependence of the magnetization recorded at 2 K (Figure 4, insert) indeed shows that for 50 kOe the magnetization reaches only a value of $10 \text{ N}\beta$.

The results reported here show that the association of a building block like $\{\text{Nb}(\text{CN})_8\}^{4-}$ with complexes for which the equatorial coordination sites are blocked by a macrocyclic ligand permits us to prepare nanosized molecular objects very efficiently. Interestingly, the dimensionality of the supramolecular architecture can be selectively controlled by the complementary molecular module leading in the present case either to a 1-D coordination polymer or to an octadecaheteronuclear molecule. The latter is one of the largest magnetic clusters formed by spontaneous association of complementary molecular building blocks.

From a magnetic point of view, the information gathered for compound **1** shows that the $\{\text{Mn}(\text{II})-\text{Nb}(\text{IV})\}$ interaction is antiferromagnetic. The behavior exhibited by compound **2** is much less straightforward, and no information on the actual exchange interaction between a Ni(II) ion linked to Nb(IV) by the means of a bridging CN ligand can be directly

deduced. Further investigations are required to conclude whether the observed behavior for **2** is the consequence of magnetic interactions among the clusters in the crystal lattice or if it is due to a more complicated intramolecular interaction scheme involving next-neighbor exchange interactions. Finally, it might be mentioned that compounds **1** and **2** are among the very first examples¹⁴ of compounds involving $\{\text{Nb}(\text{CN})_8\}^{4-}$ as a spin carrier.

Acknowledgment. The authors are grateful to the French Ministry of Research for providing R.P. with a research fellowship.

Supporting Information Available: Crystallographic information file (CIF) for compounds **1** and **2**. This material is available free of charge via the Internet at <http://pubs.acs.org>.

IC034628X

- (14) Pilkington, M.; Decurtins, S. *Chimia* **2000**, *54*, 593–601.
 (15) Kiernan, P. M.; Griffith, W. P. *J. Chem. Soc., Dalton Trans.* **1975**, 2489–94.
 (16) Jiménez-Sandoval, O.; Ramirez-Rosales, D.; Rosales-Hoz, M. J.; Sosa-Torres, M. E.; Zamorano-Ulloa, R. *J. Chem. Soc., Dalton Trans.* **1998**, 1551–6.
 (17) Karn, J. L.; Busch, D. H. *Inorg. Chem.* **1969**, *8*, 1149–53.
 (18) Sheldrick, G. M. *Programs for Crystal Structure Analysis (Release 97-2)*; University of Göttingen: Göttingen, Germany, 1998.
 (19) Farrugia, L. J. *J. Appl. Crystallogr.* **1999**, *32*, 837.
 (20) Preparation and characterization for $\{[\text{MnL}^1]_2\{\text{Nb}(\text{CN})_8\}(\text{H}_2\text{O}) \cdot 5\text{H}_2\text{O}\}_n$, **1**: In a typical crystallization experiment in a test tube (total volume ca. 40 mL), a solution of $[\text{K}_4\text{Nb}(\text{CN})_8 \cdot 2\text{H}_2\text{O}]^{15}$ (37 mg, 0.075 mmol) was allowed to slowly diffuse into a H_2O solution of $\{\text{MnL}^1\}-\text{Cl}_2$ ¹⁶ (77 mg, 0.15 mmol) yielding **1** (50 mg, yield = 31%) as light-orange needles; these crystals were suitable for X-ray analysis. Anal. Calcd for $\text{C}_{38}\text{H}_{55}\text{N}_{18}\text{O}_6\text{Mn}_2\text{Nb}$: C, 42.95; H, 5.21; N, 23.72. Found: C, 43.05; H, 5.05; N, 23.58. IR (KBr pellet, cm^{-1}) ν_{CN} : 2122(sh), 2113 (s). $\{[\text{NiL}^2]_{12}\{\text{Nb}(\text{CN})_8\}_6(\text{H}_2\text{O})_6\} \cdot 100\text{H}_2\text{O}$, **2**, was obtained by the same procedure starting from $[\text{K}_4\text{Nb}(\text{CN})_8 \cdot 2\text{H}_2\text{O}]$ (37 mg, 0.075 mmol) and $\{\text{NiL}^2\}(\text{ClO}_4)_2$ ¹⁷ (77 mg, 0.15 mmol). After a period of two weeks, needle shaped dark amber crystals of **2** (50 mg, yield = 53%) were collected. Anal. Calcd for $\text{C}_{228}\text{H}_{476}\text{N}_{96}\text{O}_{106}\text{Ni}_{12}\text{Nb}_6$: C, 36.41; H, 6.38; N, 17.88. Found: C, 36.60; H, 5.48; N, 18.01. IR spectra (KBr pellet, cm^{-1}) ν_{CN} : 2153(w), 2129(sh), 2111(m).
 (21) Crystal and structure refinement parameters for $\{[\text{MnL}^1]_2\{\text{Nb}(\text{CN})_8\}(\text{H}_2\text{O}) \cdot 5\text{H}_2\text{O}\}_n$, **1** follow: $\text{C}_{38}\text{H}_{55}\text{N}_{18}\text{O}_6\text{Mn}_2\text{Nb}$, $M = 1065.81$, crystal size $0.35 \times 0.10 \times 0.10 \text{ mm}^3$, Nonius κ -CCD, crystal to detector distance 35 mm, 110 s per frame, 1° per frame rotation, $T = 150(2) \text{ K}$, monoclinic, $a = 12.997(5) \text{ \AA}$, $b = 17.182(5) \text{ \AA}$, $c = 20.836(5) \text{ \AA}$, $\beta = 92.16(1)^\circ$, $V = 4820(3) \text{ \AA}^3$, space group $P2_1/c$, $Z = 4$, $\mu(\text{Mo K}\alpha) = 0.812 \text{ mm}^{-1}$, θ range for data collection $3.4\text{--}6.4^\circ$, 99.5% completeness, 26510 collected reflns, 9823 unique ($R_{\text{int}} = 0.043$). The structural determination by direct methods and the refinement of atomic parameters based on full-matrix least-squares on F^2 were performed using the SHELX-97¹⁸ programs within the WINGX package.¹⁹ There were 586 refined parameters. Final quality refinement criterion: $R(\text{obs}) = 0.082$, $wR2(F^2) = 0.210$, $(\Delta/\sigma)_{\text{max}} = 0.002$. GOF on F^2 : 1.02. Largest diff peak and hole $1.66/-1.34 \text{ e \AA}^{-3}$. $\{[\text{NiL}^2]_{12}\{\text{Nb}(\text{CN})_8\}_6(\text{H}_2\text{O})_6\} \cdot 100\text{H}_2\text{O}$, **2**: $\text{C}_{114}\text{H}_{147}\text{N}_{48}\text{O}_{10}\text{Ni}_6\text{Nb}_3$, $M = 2980.79$, crystal size: $0.60 \times 0.05 \times 0.05 \text{ mm}^3$, Nonius κ -CCD, crystal to detector distance 35 mm, 350 s per frame, 1° per frame rotation, $T = 150(2) \text{ K}$, trigonal, $a = 33.233(10) \text{ \AA}$, $c = 25.275(5) \text{ \AA}$, $V = 24173(11) \text{ \AA}^3$, space group $R\bar{3}$, $Z = 6$, $\mu(\text{Mo K}\alpha) = 0.950 \text{ mm}^{-1}$. All samples investigated show a very bad diffraction pattern with no observed data at angle higher than a θ angle of 20° , 8768 collected reflns, 4055 unique ($R_{\text{int}} = 0.14$). There were 517 refined parameters. Final quality refinement criterion: $R(\text{obs}) = 0.112$, $wR2(F^2) = 0.264$, $(\Delta/\sigma)_{\text{max}} = 0.000$. GOF on F^2 : 1.01. Largest diff peak and hole $1.09/-0.66 \text{ e \AA}^{-3}$.